

Transition to Lamellar-Catenoid Structure in Block-Copolymer Melts

M. Olvera de la Cruz,* A. M. Mayes, and B. W. Swift

Department of Materials Science & Engineering, Northwestern University, Evanston, Illinois 60208

Received July 13, 1991; Revised Manuscript Received August 28, 1991

ABSTRACT: The microphase transition in symmetric and nearly symmetric diblock-copolymer melts is studied expanding the density of the periodic structures in multiple harmonics. We analyze the periodicity in the weak segregation regime minimizing the Landau mean field free energy of the structure. The density distribution inside the unit cell is constructed for various morphologies. A three-dimensional hexagonal structure, identified as a "lamellar-catenoid", is found to be the equilibrium structure at the transition. It consists of alternating lamellar domains connected by an orthogonal array of hexagonally packed cylinders.

I. Introduction

Block-copolymer melts have unique morphological features. A net repulsive interaction between the A and B monomers ($\chi > 0$) of the chemically linked A and B chains drives the system to segregate locally.¹⁻⁸ The degree of polymerization N , the block-copolymer composition $f = N_A/N$, and the Flory interaction parameter χ ($\sim 1/T$) determine the physical properties of the melt. When χN is small the block-copolymer melt is isotropic. At $\chi N = (\chi N)_t$ a disorder-order transition occurs, known as the microphase separation transition (MST). At the MST the chains segregate into A-rich and B-rich domains that form periodic arrays termed microphases.

The observed microphase morphology in the strong segregation regime² ($\chi N \gg (\chi N)_t$) are alternating lamellar domains (lam), hexagonally packed cylinders (hpc), body-centered cubic packed spheres (bcc), and bicontinuous double diamond nets (bdd).⁴⁻⁶ Near the transition, referred to as the weak segregation regime, a lamellar-catenoid (lc) structure has been observed experimentally.^{5,7} The lc is an array of lamellar domains connected perpendicularly by an array of hexagonally packed cylinders. The stability of a three-dimensional hexagonal structure that resembles a lc type structure was recently tested in the weak segregation limit.⁹ This structure was found to be the stable structure for symmetric and nearly symmetric diblocks. In the strong segregation limit, on the other hand, no region of stability was found for the lc structure.¹⁰

Leibler¹ analyzed the microphase transition in weakly segregated diblock-copolymer melts expanding the free energy of the isotropic state in the Fourier components of the local monomer concentration fluctuations around the mean concentration. The largest contribution to the free energy at the transition is from the wave vectors of maximum scattered intensity, whose wavelength $2\pi/k^*$ is associated with the periodicity (d) of the emerging morphology. Leibler evaluated the free energy of various morphologies keeping only the wave vectors of magnitude k^* , which constitute the basis reciprocal lattice vectors of the periodic structure (identified with the first Bragg reflection). By comparing the free energies of different morphologies, Leibler constructed a phase diagram in the weak segregation regime.

Because the Leibler analysis includes only the first harmonic to characterize periodic structures, different space groups having the same first Bragg reflections are indistinguishable. For example, the first harmonic vectors that describe the bcc and the bdd structures are identical. Similarly, a two-dimensional hpc and a three-dimensional

hexagonal structure denoted by $\text{hex}_{c/a}$, where c is the length of the cylindrical axis and a is the lattice spacing in the hexagonal layer, are indistinguishable. In particular, a lamellar-catenoid structure with a hexagonal array of cylinders can be described by a $\text{hex}_{c/a}$, where the ratio c/a (not fixed in a hexagonal lattice) must be determined by minimizing the free energy. Therefore, the single harmonic approximation does not discriminate between some of the observed morphologies.

The lam, hpc, bcc, and bdd structures were recently studied including the contribution of the higher harmonics in the free energy of the periodic structures.⁸ The bdd was not distinguishable as a stable structure in the weak segregation regime. The phase diagram was found to be very similar to that obtained by Leibler. When the $\text{hex}_{c/a}$ structure is included,⁹ however, minimizing the free energy with respect to the k^* and the c/a ratio, one finds that the $\text{hex}_{\sqrt{3}}$ has the lowest energy between $f = 0.5$ and $f = 0.52$ in the weak segregation regime.

The degree of segregation in a given morphology is obtained from the minimized values of k^* and the amplitudes and phase factors of the harmonics. In this paper we construct the density distribution in the unit cell for various periodic structures as a function of $\chi N > (\chi N)_t$. We analyze the lam, square, hpc, $\text{hex}_{\sqrt{3}}$, fcc, bcc, and simple cubic structures in the weak segregation regime.

II. Theory

Leibler¹ studied nearly continuous transitions from an isotropic state to a periodic structure in block copolymer melts using a Landau mean field approximation. The transition is analyzed expanding the free energy of the isotropic state in a power series of the local concentration fluctuations of A monomers $\delta\rho(r)$, around the mean concentration f (in incompressible block-copolymer melts the fluctuations of B monomers $\delta\rho_B(r) = -\delta\rho(r)$),¹ where

$$\begin{aligned} \Delta F(\rho_k)/kT = & (1/2!) \Sigma \rho_k \rho_{-k} / S_0(k) + \\ & (1/3!) \Sigma \Gamma_3(k, k', k'') \rho_k \rho_{k'} \rho_{k''} \delta(k + k' + k'') + \\ & (1/4!) \Sigma \Gamma_4(k, k', k'', k''') \rho_k \rho_{k'} \rho_{k''} \rho_{k'''} \delta(k + k' + k'' + k''') \end{aligned} \quad (1)$$

ρ_k are the Fourier components of $\delta\rho(r)$. The $S_0(k)$, $\Gamma_3(\{k\})$, and $\Gamma_4(\{k\})$ are functions of the bare two-, three-, and four-monomer correlation functions G_{ij} , G_{ijk} , and G_{ijkl} , ($i, j, k, l = A, B$) calculated by the random phase approximation method (RPA).^{1,3}

In block copolymers, as in most systems undergoing transitions to periodic structures, $S_0^{-1}(|k|)$ has a minimum

Table I
Harmonic Vectors for Three-Dimensional Periodic Structures^a

hex _{c/a}			bcc			fcc			simple cubic		
(hkl)	<i>n_i</i>	<i>α_i</i>	(hkl)	<i>n_i</i>	<i>α_i</i>	(hkl)	<i>n_i</i>	<i>α_i</i>	(hkl)	<i>n_i</i>	<i>α_i</i>
(101̄0)	3	1	(110)	6	1	(111)	4	1	(100)	3	1
(0002)	1	√3/ <i>c/a</i>	(200)	3	√2	(200)	3	√4/3	(110)	6	√2
(112̄0)	3	√3	(211)	12	√3	(220)	6	√8/3	(111)	4	√3
(202̄0)	3	2	(220)	6	2	(311)	12	√11/3	(200)	3	2
						(222)	4	2			

^a The vector (0004) in the hex_{c/a} was not included because its amplitude is nearly 0 at $f \sim 0.5$. It is equivalent to the second harmonic in a lam structure which gives zero contribution to the free energy at $f = 0.5$, as required by symmetry.

at a single wave vector magnitude k_0^* .¹¹ In the RPA, $S_0(k)$ in block-copolymer melts is the scattering intensity in the disordered state:¹

$$1/S_0(k) = Q(x)/N - 2\chi \quad (2)$$

where $x = k^2 N l^2 / 6$ and N is the number of segments of length l (for simplicity we assume here $l_A = l_B$) per chain. Since $Q(x)$ has a minimum at $x = x_0^*$, $S_0(k)$ has a peak at k_0^* which is independent of χ . The peak position, a function of f , scales as $k_0^*(f) \sim 1/R_0$, where R_0 is the unperturbed radius of gyration $R_0 = (N/6)^{1/2} l$. For $f = f_c = 0.5$ (when $\Gamma_3 = 0$), $S_0(k)$ diverges at $(\chi N)_c = Q(\chi_0^*(f_c))/2 = 10.495$, leading to an instability of the isotropic state to density fluctuations of wavelength $2\pi/k_0^*$. The $\Gamma_3(\{k\})$ and $\Gamma_4(\{k\})$ in (1) wave vector dependent functions defined as¹

$$\Gamma_3(k, k', k'') = G_{ijk}(k, k', k'') [G_{i1}^{-1}(k) - G_{i2}^{-1}(k)] \times [G_{j1}^{-1}(k') - G_{j2}^{-1}(k')] [G_{k1}^{-1}(k'') - G_{k2}^{-1}(k'')] \quad (3)$$

$$\Gamma_4(k, k', k'', k''') = \gamma_{ijkl} [G_{i1}^{-1}(k) - G_{i2}^{-1}(k)] [G_{j1}^{-1}(k') - G_{j2}^{-1}(k')] \times [G_{k1}^{-1}(k'') - G_{k2}^{-1}(k'')] [G_{l1}^{-1}(k''') - G_{l2}^{-1}(k''')] \quad (4)$$

where

$$\gamma_{ijkl} = G_{ijm}(k, k', k+k'') G_{mn}^{-1}(k+k') G_{klm}(k'', k''', k+k') + G_{ilm}(k, k''', k+k'') G_{mn}^{-1}(k+k'') G_{jkn}(k', k'', k+k''') + G_{ikm}(k, k'', k+k'') G_{mn}^{-1}(k+k'') G_{ijn}(k', k''', k+k'') - G_{ijkl}(k, k', k'', k''')$$

and G_{ij}^{-1} is the ij component of the inverse matrix of the bare two-monomer correlation functions G .

At the transition $\delta\rho(r)$ has the symmetry of the periodic structure. It can therefore be expanded in plane waves whose vectors are the reciprocal lattice vectors of the periodic structure, the compositional harmonics.¹¹ The largest contribution to the free energy in nearly continuous transitions ($\Gamma_3 \sim 0$) is from the first harmonic vectors¹² $|K_r^{(1)}| = k^* r = 1, \dots, n_1$, where n_1 is the number of nearest-neighbors (nn) in the reciprocal lattice. The distance between nn planes in the structure is $d = 2\pi/k^*$. Since higher harmonic vectors $i > 1$ generally have larger magnitudes, $|K_r^{(i)}| = \alpha_i k^*$, $r = 1, \dots, n_i$, with $\alpha_i > 1$ (Table I), their contribution is often neglected.^{1,12} The hex_{c/a} structure with indices (hkl) , $l = 2n$ ($i = -(h+k)$), and distance between planes $d(hkl) = \{4(h^2 + k^2 + hk)/3a^2 + l^2/c^2\}^{-1/2}$, however, can have first and second harmonic vectors with equal magnitudes when the c/a ratio is minimized. When the "close-packed" ratio $c/a = \sqrt{8/3}$ is used, $|K_1^{(2)}| = 1.0607k^*$. When $c/a = \sqrt{3}$, however, $|K_r^{(1)}| = |K_1^{(2)}| = k^*$ (Table I), leading to lower free energies close to the continuous transition.

Recently Marques and Cates¹³ included up to the second harmonic in systems described by a phenomenological free

energy with wave vector independent constants Γ_3 and Γ_4 , and $S_0^{-1}(|k|) = \tau + (|k| - k^*)^2$. They did not find new structures around the critical point (at $\tau = 0$, when $\Gamma_3 = 0$) because they did not studied three-dimensional hexagonal structures. When the hex_{c/a} is included in the analysis,^{9b} we found it to be more favorable than the lam, and that the hpc in some regions of the phase diagram τ/Γ_4 versus $|\Gamma_3|/\Gamma_4$. Since in block-copolymers melts Γ_3 and the Γ_4 are wave vector dependent functions of the composition, their phase diagram can be very different.^{8,9} The hex_{c/a}, for example, is more favorable than the bcc over a range of compositions, where direct transitions from isotropic to hex_{c/a} structures are observed.

We expanded $\delta\rho(r)$ up to the m th harmonic for which $|K_r^{(m)}| = 2k^*$ for various structures (when $f \sim 0.5$ the higher order harmonics $i > m$ are negligible near the transition)

$$\delta\rho(r) = \sum_{i=1}^m a_i \sum_{r=1}^{n_i} (\exp\{i(rK_r^{(i)} + \varphi_r^{(i)})\} + \text{c.c.})$$

The lam structure, for example, is described by one-dimensional vectors of magnitude $|K_1^{(i)}| = ik^*$ ($n_i = 1$), so $\alpha_i = i$ ($m = 2$). The vectors $\{k_r^{(i)}\}$, denoted by $\{i^r\}$, for a two-dimensional array of hexagonally packed cylinders (hpc) are shown in Figure 1. For this morphology $n_1 = n_2 = n_3 = 3$ with $\alpha_1 = 1$, $\alpha_2 = \sqrt{3}$, and $\alpha_3 = 2$ ($m = 3$) and $k^*/2\pi = 2/a\sqrt{3}$ (where a is the lattice spacing). The harmonic vectors of various three-dimensional structures are shown in Figure 2 and their values of n_i and α_i are listed in Tables I.

Replacing the wave vector summations in (1) by sums over the allowed vectors in (2) one obtains

$$\Delta F/KT = \sum_{i=1}^m n_i S_0^{-1}(\alpha_i k^*) a_i^2 + \sum_{ijk} (\Gamma_3)_{ijk} a_i a_j a_k / 3! + \sum_{ijkl} (\Gamma_4)_{ijkl} a_i a_j a_k a_l / 4!$$

The constraint $\delta(k+k'+k'')$ in the cubic term in (1) dictates that contributions to $(\Gamma_3)_{ijk}$ in (3) are possible only when the three vectors from the i th, j th, and k th harmonics add to 0; i.e., when three-vector circuits of the form $\pm K_s^{(i)} \pm K_t^{(j)} \pm K_u^{(k)} = 0$ are allowed in the structure. Similarly, to have a contribution $(\Gamma_4)_{ijkl} \neq 0$, four-vector circuits of the form $\pm K_r^{(i)} \pm K_s^{(j)} \pm K_t^{(k)} \pm K_u^{(l)} = 0$ are required. Since the dependence of $\Gamma_3(K_s^{(i)}, K_t^{(j)}, K_u^{(k)})$ and $\Gamma_4(K_r^{(i)}, K_s^{(j)}, K_t^{(k)}, K_u^{(l)})$ on the angles between the harmonic vectors is very small,⁸ they can be approximated to functions of their magnitudes setting $\Gamma_3(\alpha_i k^*, \alpha_j k^*, \alpha_k k^*) = \Gamma_3[(\alpha_i^2 + \alpha_j^2 + \alpha_k^2)/3]^{1/2} k^*$ and $\Gamma_4(\alpha_i k^*, \alpha_j k^*, \alpha_k k^*, \alpha_l k^*) = \Gamma_4[(\alpha_i^2 + \alpha_j^2 + \alpha_k^2 + \alpha_l^2)/3]^{1/2} k^*$ where $\Gamma_3(k)$ and $\Gamma_4(k) = \Gamma_4(0,0)_k$ are defined in refs 1 and 8 (they are both linear functions of k^2 for $|k| > k_0^*$ which slope increases as f increases; for example, for $f = 0.5$ the slope of $\Gamma_3(k)$ is zero and the slope of $N\Gamma_4(k)$ versus $(kR_0)^2$ is approximately

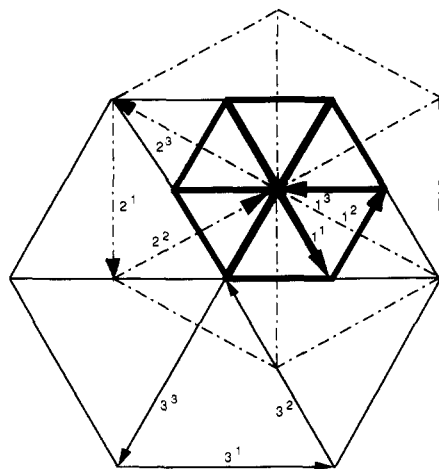


Figure 1. The hpc harmonic vectors $\{K_r^{(i)}\} = \{i^r\}$ $r = 1, \dots, n_i$, with $n_i = 3$ for $i = 1, 2$, and 3 , and $\alpha_1 = 1$, $\alpha_2 = \sqrt{3}$, and $\alpha_3 = 2$ ($m = 3$).

50). With this simplification,

$$(\Gamma_3)_{ijk} = \Gamma_3[(\alpha_i^2 + \alpha_j^2 + \alpha_k^2)/3]^{1/2} k^* A_{ijk}$$

and

$$(\Gamma_4)_{ijkl} = \Gamma_4[(\alpha_i^2 + \alpha_j^2 + \alpha_k^2 + \alpha_l^2)/3]^{1/2} k^* B_{ijkl}$$

where A_{ijk} and B_{ijkl} are numerical factors evaluated counting the possible combinations of harmonic vectors that add to zero, weighted by the phase factors. For example, A_{111} in the hpc structure is evaluated by counting the closed circuits formed with the $\{K_r^{(1)}\}_{r=1,2,3} = \{(1,0), (0,1), (1,1)\}$ vectors (see Figure 1): there are six ways of arranging these vectors to sum to zero, plus six ways for their c.c., so $A_{111} = 12 \cos(\varphi_1^{(1)} + \varphi_2^{(1)} + \varphi_3^{(1)})$. On the other hand, counting the circuits of the form $\pm K_r^{(1)} \pm K_s^{(1)} \pm K_t^{(2)} = 0$ in the hpc, we obtain $A_{112} = 12 \cos(\varphi_2^{(1)} - \varphi_1^{(1)} + \varphi_1^{(2)}) + 12 \cos(\varphi_3^{(1)} - \varphi_2^{(1)} + \varphi_2^{(2)}) + 12 \cos(\varphi_2^{(1)} - \varphi_3^{(1)} + \varphi_3^{(2)})$, and so on. The terms B_{ijkl} are evaluated by counting the four-vector circuits with their corresponding phase factors.

The resulting free energy (3) is minimized with respect to the phases $\{\varphi_r^{(i)}\}$. In centrosymmetric structures the phases are 0 or π . This agrees with the phase minimization, since it leads to the largest or smallest possible A_{ijk} and B_{ijkl} values. Furthermore, the phases within a harmonic are all equal, $\{\varphi_r^{(i)}\} = \varphi_i$ for $r = 1, \dots, n_i$. Therefore, only the phase shift between harmonics (or the "sign") needs to be determined.

We obtained the amplitudes that minimize the free energy $\{a_i\}$, for a given set of $\{\varphi_i\}$, $i = 1, \dots, m$, for each structure, and evaluated $\Delta F(\{a_i\}, \{\varphi_i\})/KT$. Phase diagrams are constructed finding the structure with lowest energy. The phase shifts for the first three harmonics are $\varphi_1 = \pi$ and $\varphi_2 = \varphi_3 = 0$ for the hpc and bcc, while $\varphi_1 = \varphi_2 = \pi$ and $\varphi_3 = 0$ for the lam, square, $\text{hex}_{c/a}$, simple cubic, and fcc when $\Gamma_3 > 0$ ($f > 0.5$); all phases shift by π (opposite "sign") when $\Gamma_3 < 0$ ($f < 0.5$). The coefficients A_{ijk} and B_{ijkl} for the first three harmonics for $\Gamma_3 < 0$ ($f < 0.5$) are given in Table II.

III. Results

The resulting free energy $\Delta F(\{a_i\}, \{\varphi_i\})/KT$ for each morphology when multiplied by N is only a function of $x^* = k^* R_0^2$ due to the scaling properties of $NS_0^{-1}(k)$, $N\Gamma_3(\{k\})$, and $N\Gamma_4(\{k\})$ with N . In the isotropic phase, away from the transition $x^* = x_0^*$, a constant independent of χ and N , so $k^* = k_0^*(f) \sim 1/R_0$. In the periodic structures

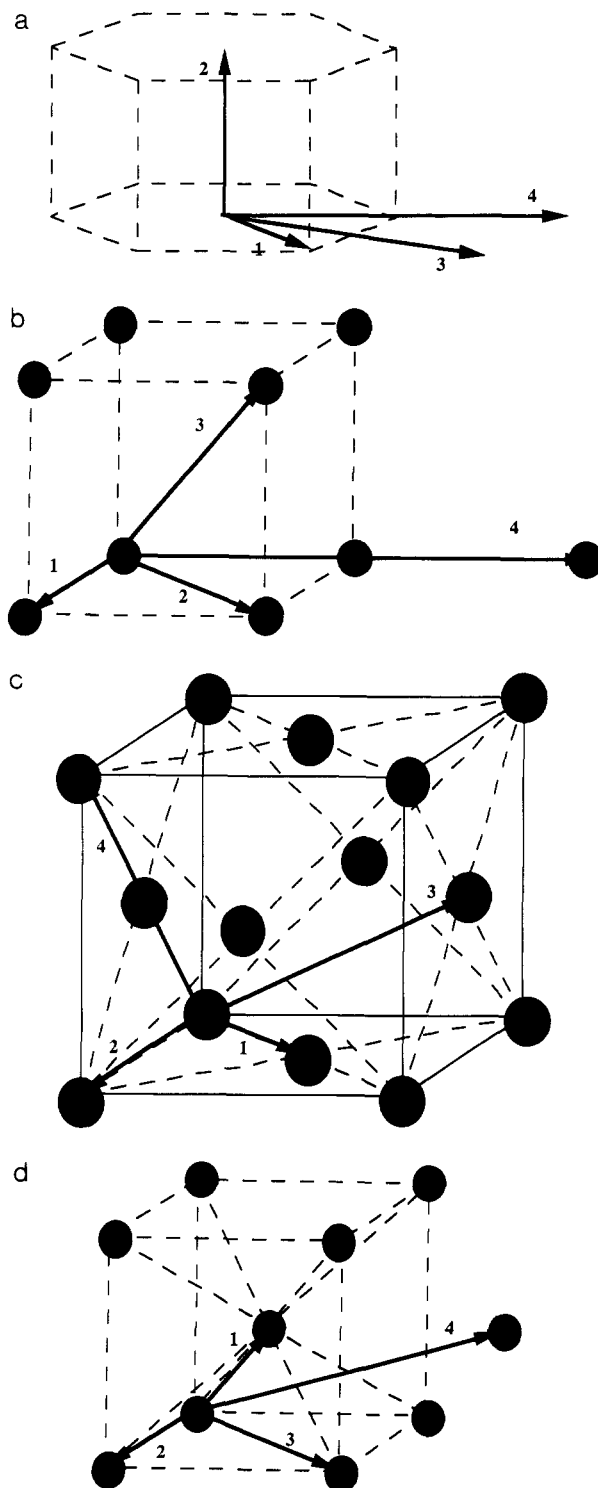


Figure 2. The harmonic vectors for (a) $\text{hex}_{c/a}$, (b) simple cubic, (c) bcc, and (d) fcc structures.

the chains are perturbed from their Gaussian coil dimensions. A further minimization of the free energy $N\Delta F(\{a_i\}, \{\varphi_i\})/KT$ with respect to x^* for each morphology is therefore required, giving the periodicity $d = 2\pi/k^*$, as a function of χ and N .^{9,14}

The phase diagram χN versus f after this minimization is shown in Figure 3. The results differ significantly from the ones obtained by Leibler¹ even if only harmonics of magnitude k^* are included. In particular, the lam and hpc are not found when the $\text{hex}_{c/a}$ phase is included in the analysis. In a recent letter^{9a} we included the fluctuations, important for finite N , self-consistently in the multiharmonic analysis following Brazovskii's¹⁵ Hartree approx-

Table II
Numerical Factors A_{ijk} and B_{ijk} for Various Periodic Structures^a

	lam	hpc	hex _{c/a}	bcc	fcc	simple cubic
A_{111}	0	12	12	48	0	0
A_{222}	0	-12	0	0	0	48
A_{333}	0	-12	-12	-48	-48	0
A_{112}	6	-36	0	-72	72	72
A_{113}	0	-18	-36	-144	-72	0
A_{133}	0	0	0	144	0	0
A_{223}	0	0	0	0	-72	0
A_{233}	0	0	0	-144	0	0
A_{123}	-12	72	0	144	0	-144
B_{1111}	6	90	90	540	216	90
B_{2222}	6	90	6	90	90	540
B_{3333}	6	90	90	2376	540	216
B_{1122}	24	360	72	576	576	1152
B_{1133}	24	288	360	4752	1152	432
B_{2233}	24	288	72	1296	1152	1296
B_{1123}	0	288	0	2304	-1440	0
B_{1223}	-24	-432	0	-1152	0	-1728
B_{1233}	0	-288	0	-2880	0	0
B_{1112}	0	-144	0	-576	0	0
B_{1113}	-8	-144	-144	-1728	0	-192
B_{1333}	0	0	0	-3456	0	0
B_{2333}	0	0	0	1152	0	0

^a $A_{122} = 0$, $B_{1222} = 0$, and $B_{2223} = 0$ for all structures.

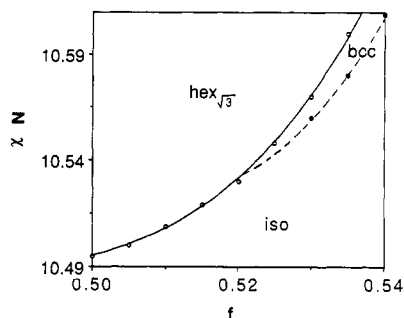


Figure 3. The diblock phase diagram, symmetric around $f = 0.5$, showing transitions to hex_{√3} (—) and to bcc (---).

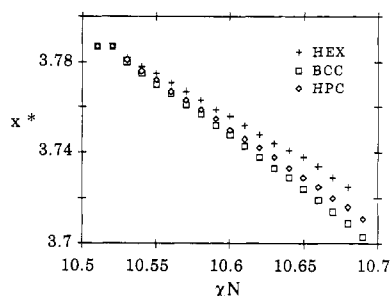


Figure 4. The value of $x^* = (k^*R_0)^2$ versus χN for various structures of $f = 0.52$.

imation. The stability of the hex_{c/a} was studied using the "close-packed" ratio $c/a = \sqrt{8/3}$ (the hex_{√8/3} is denoted by hpc in ref 9a).¹⁶ The hex_{√8/3} structure was obtained only when $N < 10^9$. Minimizing the c/a ratio instead leads to hex_{c/a} equilibrium structures even when $N \rightarrow \infty$, where the Landau mean field approximation is correct. Fixing $c/a = \sqrt{8/3}$ leads to large chain stretching, $k^* \ll k_0^*$; when $c/a = \sqrt{3}$ the chains relax and the free energy is lower than the lam and hpc free energies.

The minimized $x^* = k^*Na^2/6$ versus χN for various morphologies at $f = 0.52$ is plotted in Figure 4. The deviations in x^* from x_0^* for the lam, hpc, hex_{√3}, bcc, and simple cubic are very small (for the fcc, on the other hand, we found $x^* \gg x_0^*$). The shift in x^* to smaller values indicates chain stretching in the weak segregation regime in agreement with the experimental observations.¹⁷ When

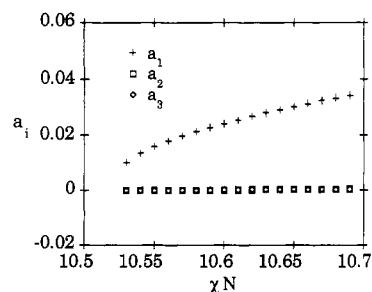


Figure 5. The amplitudes a_1 , a_2 , and a_3 as a function of χN for $f = 0.52$ in the hpc structure.

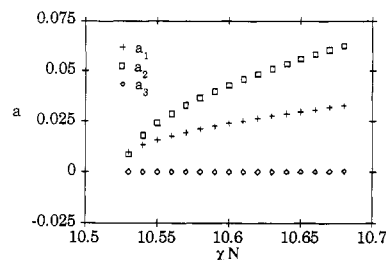


Figure 6. The amplitudes a_1 , a_2 , and a_3 as a function of χN for $f = 0.52$ in the hex_{√3} structure.

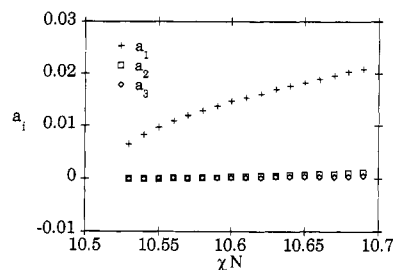


Figure 7. The amplitudes a_1 , a_2 , and a_3 as a function of χN for $f = 0.52$ in the bcc structure.

the fluctuations are self-consistently included in the analysis a shift in x^* is induced for finite N even in the isotropic state as the transition is approached,^{9a} and in the bcc structure $x^* < x_0^*$ near the MST for $f > 0.6$, suggesting a contraction of the chains in the bcc structure in agreement with some experimental observations¹⁸ and with Semenov's results.^{2b}

In Figures 5–7 we show the amplitudes a_1 , a_2 , and a_3 in the hpc, hex_{√3}, and bcc structures, respectively, for $f = 0.52$ as a function of χN . At the transition to hex_{√3} we find $a_1/a_2 \sim 1$ for $f \sim 0.52$ ($a_1/a_2 < 1$ for $0.51 < f < 0.5$), as χN increases we observe $a_1/a_2 < 1$. Also, although in the hex_{√3} we find $a_4 \sim a_3$ for $f \sim 0.52$, when f increases $a_4 \gg a_3$ because $a_3 \rightarrow 0$ at the transition (a similar trend is observed for a_2 as f increases in the hpc and bcc structures). The approach, however, breaks down when f increases since the higher order harmonics neglected in (2) give large contributions to the free energies, and higher order terms in (1) are neglected. For $f \sim 0.5$, however, the higher harmonics $a_i, i > 2$, are orders of magnitude smaller than a_1 in all of the structures studied here.

The density distribution inside the unit cell can be constructed from the values of $k^* = x^{*1/2}/R_0$, $\{a_i\}$ and $\{\phi_i\}$ ($i = 1, \dots, m$) that minimize the periodic structure free energy. In Figures 8 and 9 we show the density in the hpc and hex_{√3} unit cells for diblocks with $f = 0.52$ along the (1010) and the (0002) planes, respectively. These figures reveal that the hex_{c/a} consists of lamellar domains connected by an orthogonal array of hexagonally packed cylinders rich in A, in a matrix rich in B. For the symmetric composition $f = 0.5$ the density rich in B has the same distribution as

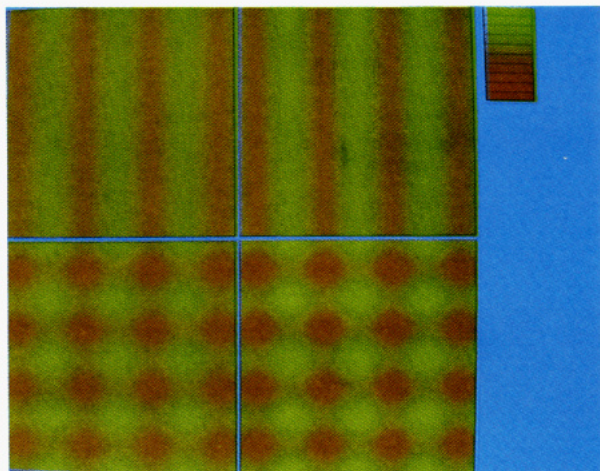


Figure 8. The density in the hpc (upper row) and in the $\text{hex}\sqrt{3}$ (lower row) unit cells for diblocks with $f = 0.52$ along the (1010) plane for $\chi N = 10.6$ (right column) and $\chi N = 10.68$ (left column). The tone bar represents the concentration of A and B monomers: the tone at the top is pure A, and at the bottom is pure B.

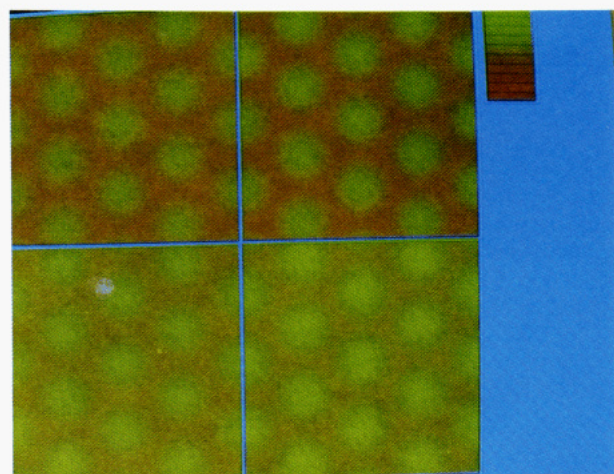


Figure 9. The density in the hpc (upper row) and in the $\text{hex}\sqrt{3}$ (lower row) unit cells for diblocks with $f = 0.52$ along the (0002) plane at $\chi N = 10.6$ (right column) and at $\chi N = 10.68$ (left column). The tone bar represents the concentration of A and B monomers: the tone at the top is pure A, and at the bottom is pure B.

the density rich in A; i.e., the structure must consist of lamellar domains of A perforated by cylinders of B alternated with lamellar domains of B perforated by cylinders of A, resembling the lamellar-catenoid structure observed by Thomas et al.⁵ The cylinders are hexagonally packed. Since for $f = 0.5$ the $\text{hex}\sqrt{3}$ should display 3-fold symmetry, the crystal system is trigonal (further analysis is required to determine the space group). When f increases, however, the density distribution in the B-rich (minority component) cylinders fades away. Therefore, for larger f the lamellar domains of A might not be perforated by cylinders (i.e., only the lamellar domains of the minority component are perforated by cylinders). A similar "lamellar-catenoid" structure was recently found experimentally,⁷ although the packing arrangement of the cylinders perpendicular to the lamellar domains has not yet been determined experimentally. In Figure 10 we show the density in the bcc unit cell along the (100) and (110) planes for $f = 0.52$.

We conclude that in block copolymer melts undergoing nearly continuous transitions to periodic structure a three dimensional hexagonal structure ($\text{hex}\sqrt{3}$) has lower free energy than the lam, square, hpc, bcc, fcc, and simple cubic when $0.47 < f < 0.52$. A multiple harmonic analysis

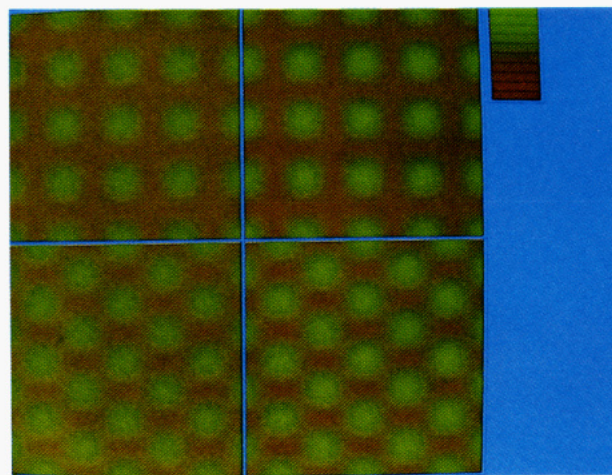


Figure 10. The density in the bcc unit cell along the (100) plane (upper row) and along the (110) plane (lower row) for diblocks with $f = 0.52$ along the at $\chi N = 10.6$ (right column) and at $\chi N = 10.68$ (left column). The tone bar represents the concentration of A and B monomers: the tone at the top is pure A, and at the bottom is pure B.

allows one to obtain the density distribution inside the unit cell in the weak segregation limit.

Acknowledgment. M. Olvera de la Cruz thanks M. E. Cates, B. Crist, A. Mondragon, and E. L. Thomas for helpful discussions. This work was supported by the David and Lucile Packard Foundations, the Alfred P. Sloan Foundation, and NSF under grant no. DMR9057764.

References and Notes

- (1) Leibler, L. *Macromolecules* **1980**, *13*, 1602.
- (2) (a) Helfand, E. *Macromolecules* **1975**, *8*, 552. (b) Semenov, A. N. *Zh. Eksp. Teor. Fiz* **1985**, *88*, 1242 (*Sov. Phys. JETP* **1985**, *61*, 733).
- (3) Olvera de la Cruz, M.; Sanchez, I. C. *Macromolecules* **1986**, *19*, 2501. Mayes, A. M.; Olvera de la Cruz, M. *J. Chem. Phys.* **1989**, *91*, 7228.
- (4) Hashimoto, T.; Shibayama, M.; Kawai, H. *Macromolecules* **1980**, *13*, 1237. Hashimoto, T.; Shibayama, M.; Kawai, H. *Macromolecules* **1983**, *16*, 1093. Hadziioannou, G.; Skoulios, A. *Macromolecules* **1982**, *15*, 258.
- (5) Thomas, E. L.; Anderson, D. M.; Henkee, C. S.; Hoffman, D. *Nature* **1988**, *334*, 598.
- (6) Roe, R.-J.; Fishkis, M.; Chang, J. C. *Macromolecules* **1981**, *14*, 1091.
- (7) Thomas, E. L.; Bates, F. S. Personal communications.
- (8) Mayes, A. M.; Olvera de la Cruz, M. A multiple harmonic analysis of ordered morphologies in weakly segregated block copolymer melts. Preprint, 1991. Mayes, A. M. Ph.D. Thesis, Northwestern University, 1991.
- (9) (a) Olvera de la Cruz, M. *Phys. Rev. Lett.* **1991**, *67*, 85. (b) Olvera de la Cruz, M. Hexagonal lattices in nearly continuous transitions to periodic structures. In press.
- (10) Fredrickson, G. H. *Macromolecules* **1991**, *24*, 3456.
- (11) Landau, L. D. *The Collected Papers of L. D. Landau*. Ter Haar, D., Ed.; Pergamon Press: 1965; pp 212–214.
- (12) Alexander, S.; McTague, J. *Phys. Rev. Lett.* **1978**, *41*, 702.
- (13) Marques, C. M.; Cates, M. E. *Europhys. Lett.* **1990**, *13*, 267.
- (14) Mayes, A. M.; Olvera de la Cruz, M. *Macromolecules* **1991**, *24*, 3975. Tang, H.; Freed, K. F. In Press.
- (15) Brazovskii, S. A. *Sov. Phys. JETP* **1975**, *41*, 85. Fredrickson, G. H.; Helfand, E. *J. Chem. Phys.* **1987**, *87*, 697.
- (16) Table I in reference 9a has a typographical error: $(\Gamma_3)_{112}$ for the hpc and bcc structures should be multiply by -1 .
- (17) Owens, J. N.; Gancarz, I. S.; Koberstein, J. T.; Russell, T. P. *Macromolecules* **1989**, *22*, 3380. Almdal, K.; Rosedale, J. H.; Bates, F. S.; Wignall, G. D.; Fredrickson, G. H. *Phys. Rev. Lett.* **1990**, *65*, 1112.
- (18) Bates, F. S.; Berney, C. V.; Cohen, R. E. *Macromolecules* **1983**, *16*, 1101. Richards, R. W.; Thomason, J. L. *Macromolecules* **1983**, *16*, 982.